Mechanism of Smoke Generation in a Flickering Pool Fire

Ritsu DOBASHI, Zu-Wei KONG, Akira TODA, Nobuhide TAKAHASHI,
Masataro SUZUKI and Toshisuke HIRANO

Department of Chemical System Engineering
School of Engineering
The University of Tokyo
7-3-1 Hongo, Bunkyo-ku, Tokyo 113-8656, JAPAN

ABSTRACT

Smoke generation process in a flickering pool fire was examined to understand the effect of hydrodynamic properties of the flame on smoke generation. A detailed observation was performed in a toluene pool fire with diameter of 90 mm. Smoke generation occurred when flame flickers with a mushroom-like flame appearance. As the mushroom-like flame appears, gas flow moves almost horizontally and parallel to the flame front just under the mushroom-like flame, and at the same time a large amount of smoke is released from the flame. The residence time of soot particle in the soot production region is increased by the flickering motion of the flame. Soot growth is enhanced by the increase in the residence time. The increased radiative heat loss by the grown soot particles might result in flame extinction and a large amount of smoke is released from the flame. The calculation of the velocity induced by thermophoretic force was also performed. It is found that the thermophoretic force affects on the smoke generation process in a flickering flame.

KEY WORDS: Smoke generation, Pool fire, Soot formation, Thermophoretic force, Flickering flame, Hydrodynamic property

INTRODUCTION

Smoke is often generated from sooting non-premixed flames. In the case of combustion facilities, the generated smoke causes air pollution when it is released to the ambient atmosphere. In the case of pool fires, the generated smoke strongly influences the radiative heat transfer from the pool fire. The fire plume on the pool is almost covered by heavy smoke especially when the diameter of pool becomes larger than a few meters. The radiative heat transfer from the pool fire is an important factor for safety management [1, 2]. Therefore, it is

indispensable to understand the mechanism of the smoke generation.

With increasing diameter of pool, the smoke generation rate increases by a large amount. One of the reasons for the enhancement of smoke generation might be that the available oxygen at the combustion region relative to the fuel vapor decreases as the diameter increases. The other reason considered is that the dynamic behavior of pool flame influences the process of smoke generation. It is well known that the behavior of the pool fire depends on the pool size [1-4]. As the diameter increases, the flame structure becomes unstable and the flame motion develops turbulence.

In a sooting flame, primary soot particles are formed and then the formed soot particles grow by aggregation in the soot production region. The aggregated soot particles are then oxidized in the oxidation region. If the soot particles are not burned out in the oxidation region, smoke is released to the surroundings [5]. Fuel structure and surrounding conditions influence the soot formation and smoke generation [5-7]. The hydrodynamic properties of the flame also have a major effect on these processes. Recently, some studies on soot formation were done under microgravity condition [8-11], where convective flow is suppressed and hydrodynamic properties of the flame are changed considerably. Under microgravity condition, generated soot fraction increases [8-10] and in some conditions very large soot particles appear [11]. The suspected reason for these effects are that the residence time of soot particle in the soot production region increases because of the changes in the flow structure and soot trajectory under microgravity condition.

In the flickering flames such as flames observed on large-scale pool fires, the situation similar to microgravity condition must be realized periodically. Although this situation realized for just a short period of time, this effect is expected to influence the soot formation and smoke generation processes. However, only few studies have been done to examine the effect of flame flikering on smoke generation [12]. In this study, the effect of flickering of the flame on the smoke generation was examined experimentally in detail.

EXPERIMENTAL METHODS

The schematic of experimental setting is shown in Fig. 1. The fuel pan used in this experiment is made of stainless steel with a diameter of 90 mm and a depth of 15 mm. We intended to examine the smoke generation in a flickering flame in detail. This diameter of 90 mm is large enough to generate flickering motion of flame and still small enough for detailed observation. Toluene was used as fuel because of its high soot generation rate. In the pan, water was filled up to the level of 3 mm below the edge of the rim. The fuel was then poured over the water until it was flush with the rim edge. To observe the smoke clearly, a white plate illuminated by a mercury lamp was set behind the pan. A high-speed video camera was used to record the behavior of the flame and smoke. The camera was operated at a speed of 500 frames/s.

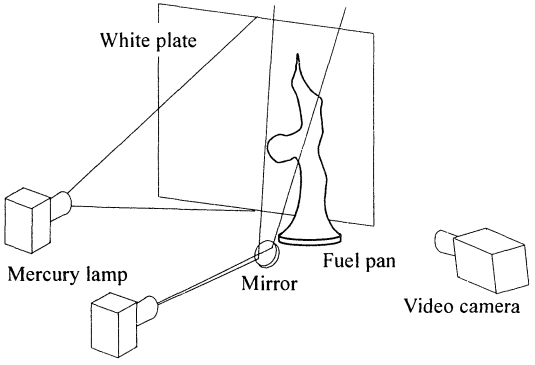

FIGURE 1 Schematic of the experimental setup.

When the flow field was examined, tracer particles were introduced in the ambient air and illuminated by a light sheet from the mercury lamp. In this observation, a normal speed (60 frames/s) video camera was used. The tracking paths of the particles during the exposure time (16.7 ms) were recorded on the image. The direction of the tracking path indicates the flow direction and the length of it indicates the velocity of flow. The tracer particles were SiO_2 with a diameter of 30 μm. Thermophoretic force would be effective for small particles located near combustion region where a steep temperature gradient exists. By our measured data of thermophoresis, the induced velocity by the thermophoretic force is estimated to be less than 2 mm/s. Therefore, the thermophoretic force may not have a significant effect on the measurement of flow field in this case.

RESULTS AND DISCUSSIONS

Behavior of Flame and Smoke Generation

Figure 2 shows a five series of entire image of fire taken at an interval of 32 ms. In the ascending path of the flame from the liquid surface to a point about 60 mm above it, the flame shape does not change remarkably. At the point about 60 mm above the liquid surface, the flame shape changes periodically and a mushroom-like flame emerges (Fig. 2 (2)). The mushroom-like flame reduces its size as it moves upwards (Fig. 2 (3), (4)). When it reaches a height of about 180 mm above the liquid surface, small pieces of flames come out from the main flame (Fig. 2 (5), (1)). They moved upward and then disappeared. On the basis of this observation, we can divide the fire plume into three regions. The first region is between liquid surface and a point about 60 mm above it. The second is between about 60 mm and about 180 mm. The third is the region higher than the point about 180 mm above the liquid surface. These regions can be called the persistent region, the intermittent region and the plume region, respectively [3, 13].

It is seen in Fig. 2 that the smoke appears mainly in the plume and intermittent regions. Most of previous studies on smoke generation have not focused on the smoke generation in the intermittent region. It was shown in our previous study [1] that in the case of large-scale pool fires the radiation from the intermittent region plays an important role and the intensity of the

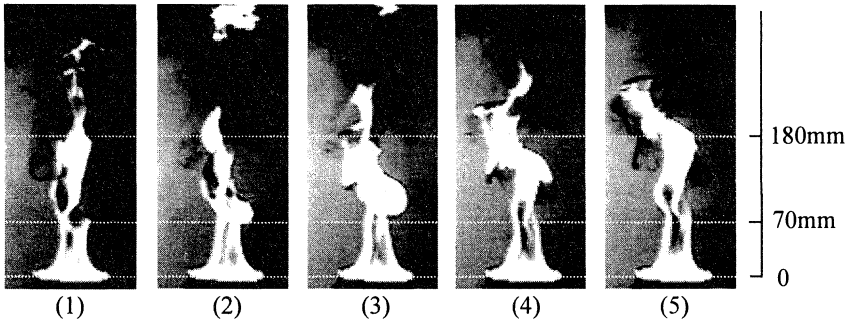

FIGURE 2 A series of images of the entire fire plume. Time interval: 32ms

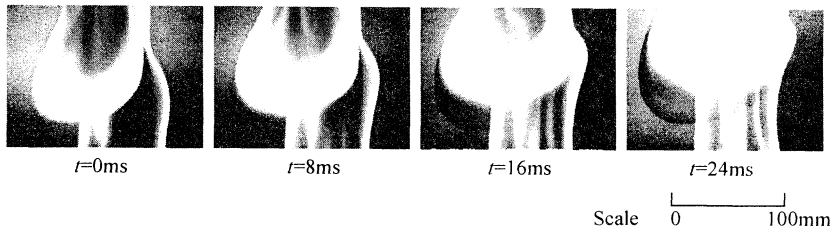

FIGURE 3 A series of the images which represent the behavior of a mushroom-like flame.

radiation closely relates to the smoke generation in this region. Therefore, the smoke generation in the intermittent region is important to appropriately understand the radiative properties from large-scale pool fires. In this study, the smoke generation from the intermittent region was focused.

Figure 3 shows a series of enlarged images of the intermittent region of the flame at an interval of 8 ms. This figure shows the images of the flame between 50 mm and 170 mm above the liquid surface. The quantity t indicates the time from the moment when the first picture of Fig. 3 was taken. In the first picture (Fig. 3, t = 0), a mushroom-like flame can be seen while the smoke can not be observed. In the second picture (Fig. 3, t = 8 ms), the mushroom-like flame moves upward and smoke appears nearly at the position where the flame was located in the first picture. In the third picture (Fig. 3, t = 16 ms), the flame continues to move upward and the generated smoke becomes more dense. In the forth picture (Fig. 3, t = 24 ms), both the flame and smoke move upward. The smoke moves more slowly than the flame. The outlines of the flame and smoke were traced at every 2 ms to examine the behavior of the flame and smoke. These traced lines were combined in one figure (Fig. 4). Figure 4 shows that the flame ascending velocity starts to increase at the position about 80 mm above the liquid surface and then smoke appears nearly at the same position. The position of the traced lines were measured and plotted against time t in Fig. 5. This position was measured as the distance from the liquid fuel surface to the flame and smoke along the vertical line 50mm leftward from the centerline of the fuel pan. The ascending velocities of the flame and smoke are calculated and plotted also in Fig.5. It is found in Fig. 5 that the ascending velocity of the flame is decreasing from 1.3 m/s (at t = -18 ms) to 0.9 m/s (at t = -8 ms), and then smoke appears at t = 2 ms nearly at the position where the flame existed at t = -6 ms. After the

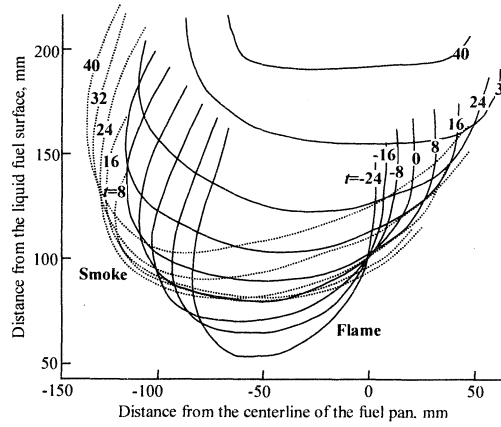

FIGURE 4 Periodic traces of the outlines of the flame and smoke.

smoke appears, the ascending velocity of the flame starts to increase and reaches about 5 m/s at t = 32ms. The generated smoke moves downward at first (t = 2-10 ms) and then upward. The ascending velocity of the smoke is increased to be 1.7 m/s at t = 20 ms and becomes almost constant value (1.7 m/s).

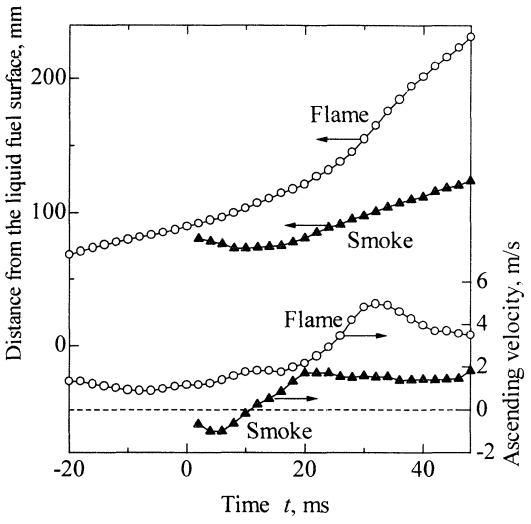

FIGURE 5 Position-time diagram of the flame and smoke.

Observation of the Flow Field

From the above observation, smoke generation rate in the intermittent region was found to be correlated with motion of the flame. In other words, the smoke generation rate is strongly influenced by the hydrodynamic properties of the flame. The flow field near the flame was examined in detail by the tracer particles, which were introduced into the ambient air. Figure 6 shows the images of the tracking paths of tracer particles. The gas flow velocity vector measured by the tracking path is also indicated in Fig. 6 (right side figures) as an arrow. In Fig. 6, side-view images of a mushroom-like flame were shown and the centerline of the pan locates at the position about 10 mm rightward from the right edge of the images. When part of flame starts to protrude (Fig. 6 (1)), gas flow moves at 0.2-0.3 m/s nearly horizontally (slightly downwardly) in the region below the protruded flame. As the protruded part becomes a mushroom-like flame, the gas flow moves at about 0.2-0.3 m/s almost horizontally in the region below the mushroom-like flame and slightly upward in the region close to the centerline (Fig. 6 (2), (3)). Even when the mushroom-like flame is ascending quickly (Fig. 6 (3)), the gas flow below the mushroom-like flame moves horizontally and the vertical component of the flow velocity is less than 0.1 m/s.

Based on the above results, the following special situation is realized for this flickering flame: the gas flow moves at a low velocity of 0.2-0.3 m/s almost horizontally along the flame front, even though the ascending gas flow of more than 1 m/s is generated in the core part of the fire plume. In this situation, soot particle stays in the soot production region, which might exist at the fuel-side of the flame front, in a relatively long time because the gas flow in this region moves almost parallel to the flame front and at relatively low velocity. This situation enhances the soot formation.

Smoke was generated after the formed soot is going out through the flame (the oxidation region). Soot is often oxidized and did not escape from the flame. It is important to understand the mechanism of soot escape because it is related to smoke generation mechanism. In the case of this study, smoke appeared when the mushroom-like flame is ascending quickly. The ascending velocity of the flame was about 5 m/s, while the vertical component of the measured flow velocity near the flame was less than 0.1 m/s. This result indicates that this rapid ascending movement of the flame is not by the ascending flow. As a diffusion flame can not move at such rapid velocity without convective effect, it is inferred that the flame was

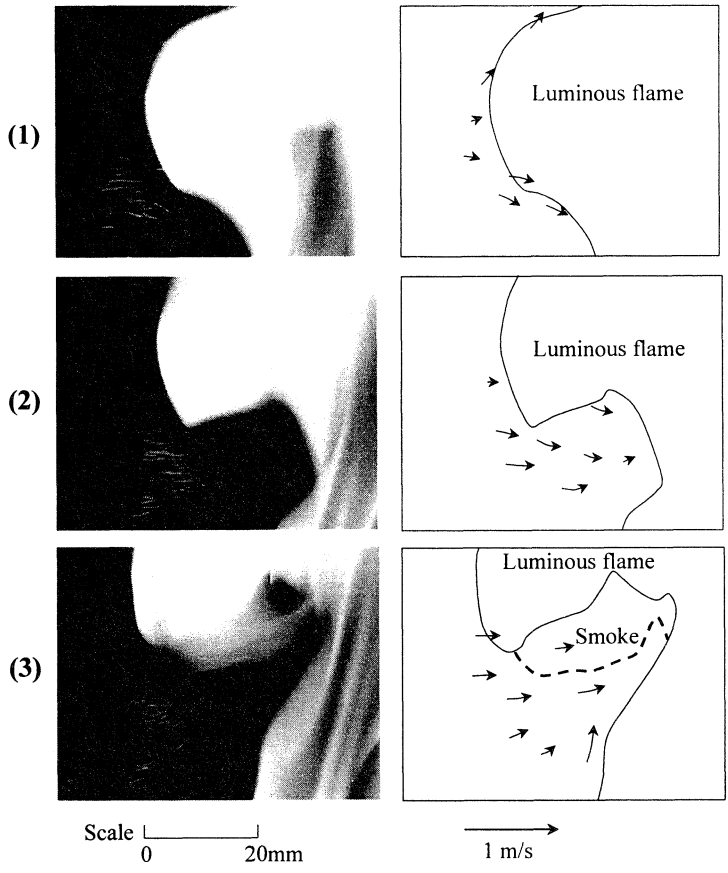

FIGURE 6 A series of images of tracking paths of the tracer particles. Time interval: 16.7 ms, Exposure time: 16.7 ms

extinguished, i.e., the extinguishing process of the edge of luminous flame could be observed as the quick ascending movement of the flame. If flame is extinguished, soot can easily escape from the flame. The radiative heat loss by the enhanced soot formation might cause the extinguishment of the flame.

Influence of Thermophoretic Force

In the field with temperature gradient, the thermophoretic force affects the motion of small particles. Near a flame where a steep temperature gradient exists, thermophoretic force may be important in affecting the process of smoke generation [14-16]. A quantitative estimation of the thermophoretic effect is attempted in this study. The thermophoretic force on smoke particle is estimated by using the results of our studies on measurements of thermophoretic

velocity under microgravity condition [14, 15]. In the experiments under microgravity condition, particle in the field with temperature gradient moves toward lower temperature side at almost constant velocity, at which velocity thermophoretic force and drag force are balanced. This velocity is called thermophoretic velocity.

On the basis of Waldmann's analysis, thermophoretic force is proportional to $\nu\nabla T/T$ in the free molecular regime [17]. The thermophoretic force F_T can be expressed by the following Equation (1).

$$F_T = -C_T(\mathrm{Kn})\nu\frac{\nabla T}{T_m}, \tag{1}$$

where C_T is a constant, which depends on the property of the particle and is a function of the Knusen number Kn (the ratio of the mean free path of ambient gas to particle radius), ν the dynamic viscosity of the ambient gas, ∇T the temperature gradient and T_m the mean temperature around the particle. The thermophoretic force is balanced with the drag force at the thermophoretic velocity U_T. The drag force can be expressed as the Stokes's law because the velocity difference between the particle and surrounding gas is small and Reynolds number around the particle is very small,

$$F_T = 6\pi\mu r U_T, \tag{2}$$

where μ is viscosity of the ambient gas and r the radius of particle. Therefore, thermophoretic velocity U_T is formulated as Equation (3).

$$U_T = -C_T(\mathrm{Kn})\frac{\nabla T}{6\pi\rho_g r T_m}, \tag{3}$$

where ρ_g is the density of the ambient gas. The data of thermophoretic velocities measured in our experiments under microgravity condition for carbon particles with the diameter of 5 μm and 15 μm are shown in Table 1. The values of C_T for these carbon particles are calculated and

TABLE 1 Measured and estimated thermophoretic velocity.

Material	Particle radius r, μm	Temperature gradient ∇T, K/mm	Mean temperature T_m, K	Gas density ρ_g, kg/m^3	Measured thermophoretic velocity U_T, mm/s	Estimated thermophoretic velocity U_T, mm/s	Constant C_T, kg/s	Knudsen number Kn, -	$C_T^{1.5}\times$Kn, $(\mathrm{kg/s})^{\frac{3}{2}}$	Remarks
Carbon	5	40	310	1.10	- 0.8		6.4×10^{-7}	0.017	8.8×10^{-12}	Measured in micro-g experiment
Carbon	15	40	310	1.10	- 0.5		1.2×10^{-6}	0.0057	7.5×10^{-12}	Measured in micro-g experiment
Carbon	0.02	200	1300	0.26		- 7.1	4.5×10^{-9}	26	8×10^{-12}	Smoke particle in the fuel side
Carbon	0.02	400	1300	0.26		- 14.1	4.5×10^{-9}	26	8×10^{-12}	Smoke particle in the air side
SiO_2	1.35	40	310	1.10	- 1.15		2.5×10^{-7}	0.063	7.8×10^{-12}	Measured in micro-g experiment
SiO_2	5	40	310	1.10	- 0.69		5.5×10^{-7}	0.017	7.0×10^{-12}	Measured in micro-g experiment
SiO_2	15	40	310	1.10	- 0.53		1.3×10^{-6}	0.0057	8.2×10^{-12}	Measured in micro-g experiment
SiO_2	15	200	1300	0.26		- 0.78	3.7×10^{-7}	0.035	8×10^{-12}	Tracer particle in the fuel side
SiO_2	15	400	1300	0.26		- 1.6	3.7×10^{-7}	0.035	8×10^{-12}	Tracer particle in the fuel side

also listed in Table 1. The diameter of the smoke particle is considered to be about 80 nm [18]. Temperature near the combustion region is assumed as 1300K. Temperature gradient near the combustion region can be assumed as 200 K/mm at the fuel side and 400 K/mm at the air side [19]. The thermophoretic velocity of the carbon particle with a diameter of 80 nm in this condition is estimated in order to assess the thermophoretic effect on soot and smoke particles. In the estimation, the value of C_T of carbon particle at Kn=26 is needed, however, this value has not measured in the experiments. The value of C_T can be roughly evaluated by using an empirical relation $C_T^{1.5} \times Kn \approx 8.0 \times 10^{-12}$ $(kg/s)^{1/2}$. As a result, the thermophoretic velocity of carbon particle with the diameter of 80 nm is estimated to be -7.1 mm/s at the fuel side and -14.1 mm/s at the air side (Table 1). The comparison between the estimated thermophoretic velocity and flow velocity is shown in Fig. 7. The thermophoretic velocity points toward cold side, therefore, thermophoretic force disturbs soot particle to pass through the flame when it is in the fuel side, and assist it to come apart from the flame when it is in the air side. Figure 7 represents that the thermophoretic force has large effect on the path of soot particle when gas flows almost parallel to the flame front. This effect might increase the residence time in the soot production region and encourage the smoke generation.

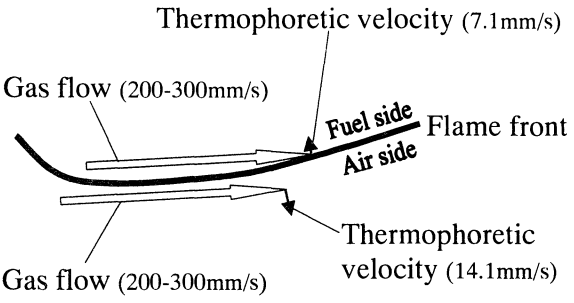

FIGURE 7 Relationship between the flow velocity and thermophoretic velocity.

The thermophoretic velocity for the tracer particle used in this study is also estimated to be -0.78 mm/s at the fuel side and -1.6 mm/s at the air side (Table 1). The effect of thermophoretic force on the tracer particles is not significant in the measurement of this study.

CONCLUSIONS

Smoke generation process in a flickering toluene pool fire of 90 mm in diameter was examined by detailed observations. The following results are derived.

1. Smoke generation is observed when flame is flickering and a mushroom-like flame appears. As the mushroom-like flame appears, gas flow moves almost horizontally and parallel to the flame front just under the flame, and then much smoke is released out of the flame.
2. The residence time of soot particle in the soot production region is increased by the flickering motion of the flame. Soot growth rate is enhanced by the increase of residence time. The increased radiative heat loss by the grown soot particles might result in flame extinction and much smoke releases out of the flame. This extinguishing process is inferred to be observed as a quick ascending movement (about 5 m/s) of the protruded flame.
3. The situation when the thermophoretic force becomes effective on the smoke generation process can be realized in a flickering flame.

REFERENCES

1. Takahashi, N., Kong, Z.W., Suzuki, M., Dobashi, R. and Hirano, T., "Behavior of Flame in Large Scale Pool Fires", Proceedings of the Second International Symposium on Scale Modeling, pp.25-32, 1997.

2. Tskahashi, N., Suzuki, M., Dobashi, R. and Hirano, T., "Behavior of Luminous Zones Appearing on Plumes of Large Scale Pool Fires", Fire Safety Journal, (in press).

3. Bouhafid, A., Vantelon, J.P., Joulain, P. and Fernandez-Pello, A.C., "On the Flame Structure at the Base of a Pool Fire", The Twenty-Second Symposium (International) on Combustion, The Combustion Institute, Pittsburgh, Pa., pp.1291-1298, 1988.

4. Choi, M.Y., Hamins, A., Rushmeier, H. and Kashiwagi, T., "Simultaneous Optical Measurement of Soot Volume Fraction, Temperature, and CO2 in Heptane Pool Fire", The Twenty-Fifth Symposium (International) on Combustion, The Combustion Institute, Pittsburgh, Pa., pp.1471-1480, 1994.

5. Puri, R., Richardson, T.F., Santoro, R.J. and Dobbins, R.A., "Aerosol Dynamic Processes of Soot Aggregates in a Laminar Ethene Diffusion Flame", Combustion and Flame, 92, pp.320-333, 1993.

6. Glassman, I., "Soot Formation in Combustion Processes", The Twenty-Second Symposium (International) on Combustion, The Combustion Institute, Pittsburgh, Pa., pp.295-311, 1988.

7. Williams, J.M. and Gritzo, L.A., "in situ Sampling and Transmission Electron Microscope Analysis of Soot in the Flame Zone of Large Pool Fire", The Twenty-Seventh Symposium (International) on Combustion, The Combustion Institute, Pittsburgh, Pa., pp.2707-2714, 1998.

8. Law, C.K. and Faeth, G.M., "Opportunities and Challenges of Combustion in Microgravity", Progress in Energy and Combustion Science, 20, pp.65-113, 1994.

9. Sunderland, P.B., Mortazavi, S. and Faeth, G.M., "Laminar Smoke Points of Nonbuoyant Jet Diffusion Flames", Combustion and Flame, 96, pp.97-103, 1994.

10. Kaplan, C.R., Oran, E.S., Kailasanath, K. and Ross, H.D., "Gravitational Effects on Sooting Diffusion Flames", The Twenty-Sixth Symposium (International) on Combustion, The Combustion Institute, Pittsburgh, Pa., pp.1301-1309, 1996.

11. Ito, H., Fujita, O. and Ito, K., "Agglomeration of Soot Particles in Diffusion Flames under Microgravity", Combustion and Flame, 99, pp.363-370, 1994.

12. Smyth, K.C., Shaddix, C.R. and Everest, D.A., "Aspects of Soot Dynamics as Revealed by Measurements of Broadband Fluorescence and Flame Luminosity in Flickering Diffusion Flames", Combustion and Flame, 111, pp.185-207, 1997.

13. Venkatesh, S., Ito, A., Saito, K. and Wichman, I.S., "Flame Base Structure of Small-Scale Pool Fires", The Twenty-Sixth Symposium (International) on Combustion, The Combustion Institute, Pittsburgh, Pa., pp.1437-1443, 1996.

14. Toda, A., Ohi, Y., Dobashi, R., Hirano, T. and Sakuraya, T., "Accurate Measurement of Thermophoretic Effect in Microgravity", Journal of Chemical Physics, 105: 16, pp.7083-7087, 1996.

15. Toda, A., Ohnishi, H., Dobashi, R., Hirano, T. and Sakuraya, T., "Experimental Study on the Relation between Thermophoresis and Size of Aerosol Particles", International Journal of Heat and Mass Transfer, 41: 17, pp.2710-2713, 1998.

16. Rosner, D.E., Mackowski, D.W. and Garcia-Ybarra, P., "Size- and Structure-Insensitivity of the Thermophoretic Transport of Aggregated "Soot" Particles in Gases", Combustion Sciend and Technology, 80, pp.87-101, 1991.

17. Waldmann, L.., "On the motion of spherical particles in nonhomogeneous gases", Rarefied Gas Dynamics (ed. by L.Talbot), Academic Press Inc., New York, 1961, pp.323-344.

18 Köylü, Ü.Ö. and Faeth, G.M., "Structure of Overfire Soot in Buoyant Turbulent Diffusion Flames at Long Residence Times", Combustion and Flame, 89, pp.140-156, 1992.

19. Pagni, P.J. and Okoh, C.I., "Soot Generation within Radiating Diffusion Flames", The Twentieth Symposium (International) on Combustion, The Combustion Institute, Pittsburgh, Pa., pp.1045-1054, 1984.